ARPA ORDER NO.: 3584
OE20 Strategic Technology

A RAND NOTE

# CONCEPTS OF SIGNAL ACQUISITION AND PROCESSING FOR USE WITH A PASSIVE SPACE COMMUNICATION ARRAY

James C. Springett

July 1980

N-1550-ARPA

Prepared For

The Defense Advanced Research Projects Agency

Rand
SANTA MONICA, CA. 90406

The research described in this report was sponsored by the Defense Advanced Research Projects Agency under Contract No. MDA903-78-C-0281.



Published by The Rand Corporation

ARPA ORDER NO.: 3584
OE20 Strategic Technology

# A RAND NOTE

# CONCEPTS OF SIGNAL ACQUISITION AND PROCESSING FOR USE WITH A PASSIVE SPACE COMMUNICATION ARRAY

James C. Springett

July 1980

N-1550-ARPA

Prepared For

The Defense Advanced Research Projects Agency

Rand
SANTA MONICA, CA. 90406

# PREFACE

The Defense Advanced Research Projects Agency (ARPA) has for several years (through 1977) supported the design and technical evaluation of a passive communications satellite (PACSAT) by the Stanford Research Institute (now SRI International). In 1977, the Defense Communications Agency (DCA) asked The Rand Corporation to examine the utility of PACSAT, as well as other passive satellite designs to support a communications link between the National Command Authority and the airborne strategic bomber force. The present study examines the use of PACSAT in a communications link to the MX mobile-missile sites. That application differs from those of the earlier Rand study in that the location of the MX missile sites is known to the transmitter, thus allowing a priori carrier frequency selection and relaxing the antenna requirements for an ideal PACSAT configuration. In addition, this study examines the performance of PACSAT for nonideal configurations.

The study reported in this Note examines the possibility of using signal processing techniques for correcting the PACSAT return signal for near-field effects and signal acquisition. The results should be of interest to analysts associated with strategic communications, planning, and operations.

James C. Springett and Irving S. Reed, the author of the appendix, are consultants to The Rand Corporation.

CONTENTS

# I. INTRODUCTION AND SUMMARY

The concept of a linear discrete element reflecting array in earth orbit as a method for providing reliable communications between highly selective geographical areas has been proposed by Yater [1]* and subsequently developed by SRI [2]. Such a passive communication satellite (PACSAT), for example, may serve to provide command communications for portions of the strategic forces. For a sufficiently large (long) PACSAT, individual sites may be addressed because the return signal beamwidth is very narrow. Addressing is accomplished by carrier frequency; the nominal requirements for such services will be covered in a companion Rand Note [3].

This Note is primarily concerned with two problems that affect efficient PACSAT system operation: (1) the need for the receiving terminal to search for the carrier frequency being employed, and (2) a method by which the full potential of the array may be realized when the receiving terminal operates in the near-field of the reflected electromagnetic radiation. The first problem results from an assumed inability of the receiving terminal to know exactly the location (in terms of incident angle to the array) of the transmitter (plus some additional uncertainty as to the possible tilt angle--relative to the ideal vertical--of the array). As a result, the receiver must search (over a limited range) for the frequency that the transmitter uses** to illuminate the receiver. The second problem results from the length of the array and the use of a low orbit altitude. Without some form of compensation processing, the individual reflected waves from each element of the array arrive at the receiving antenna with sufficient cumulative phase error that the potential gain of the array is significantly degraded.

---

*References to the main body of the text may be found on p. 37.

**The transmitter is assumed to know exactly the location of the receiver and all other essential parameter values.

A solution to the frequency search problem is to use a discrete set of frequencies spaced by an amount sufficient to steer the reflected beam by one beamwidth between any two adjacent frequencies. Thus, the transmitter selects the particular frequency that places the receiver within the return beam, and the receiver searches over a subset of the frequencies to locate that being employed.

To minimize the near-field loss, it is proposed that the carrier be modulated by a pseudo-noise (PN) code which permits subdivision of the array return into spatial segments by means of correlation techniques at the receiver. Since each spatial segment acts as a short array for which the near-field cumulative phase error is small, the mean phase differences between the segments may be corrected (removed), and the segment components combined to effect the return from the total array with an acceptably low loss.*

The following sections develop the various concepts. Section II introduces an electrical transfer function model for the array which is useful to the ensuing developments. Section III discusses the frequency acquisition process, and Section IV addresses the near-field correction processor. Finally, Section V concludes with an outline for further work.

The appendix discusses an alternate approach for a frequency detector.

---

*Compensation of this form was originally suggested by Dr. Irving S. Reed, Rand Consultant.

## II. PACSAT ARRAY TRANSFER FUNCTION MODEL

Figure 1 shows the basic geometry of the transmitter (T) and receiver (R) relative to the bottom (nearest) element of the array which is located at an altitude H above the perpendicular to the baseline TR. The distance from T to element 1 is designated $\rho_1$, and the distance from T to the nth element is $\rho_{1n}$. Similar designations are made for the R to element distances, as shown. Angles to the array are defined as indicated on Fig. 1. In total, there are N elements in the array, and each element is spaced by a distance s.

The distances are related to the altitude and the angles in the following manner.

$$\rho_1 = \sqrt{H^2 + H^2 \tan^2 \alpha} \tag{1}$$

$$\rho_{1n} = \sqrt{(H + ns)^2 + H^2 \tan^2 \alpha} \quad . \tag{2}$$

Combining (1) and (2) yields:

$$\rho_{1n} = \rho_1 \sqrt{1 + \frac{2Hns}{\rho_1^2} + \frac{(ns)^2}{\rho_1^2}} \quad . \tag{3}$$

By expanding the radical in a series, and neglecting the third order and higher terms which have no practical effect for the PACSAT, (3) becomes:

$$\rho_{1n} \cong \rho_1 + \frac{Hns}{\rho_1} + \frac{(ns)^2}{2\rho_1}\left[1 - \frac{H^2}{\rho_1^2}\right] . \tag{4}$$

Similarly,

$$\rho_{2n} \cong \rho_2 + \frac{Hns}{\rho_2} + \frac{(ns)^2}{2\rho_2}\left[1 - \frac{H^2}{\rho_2^2}\right] . \tag{5}$$

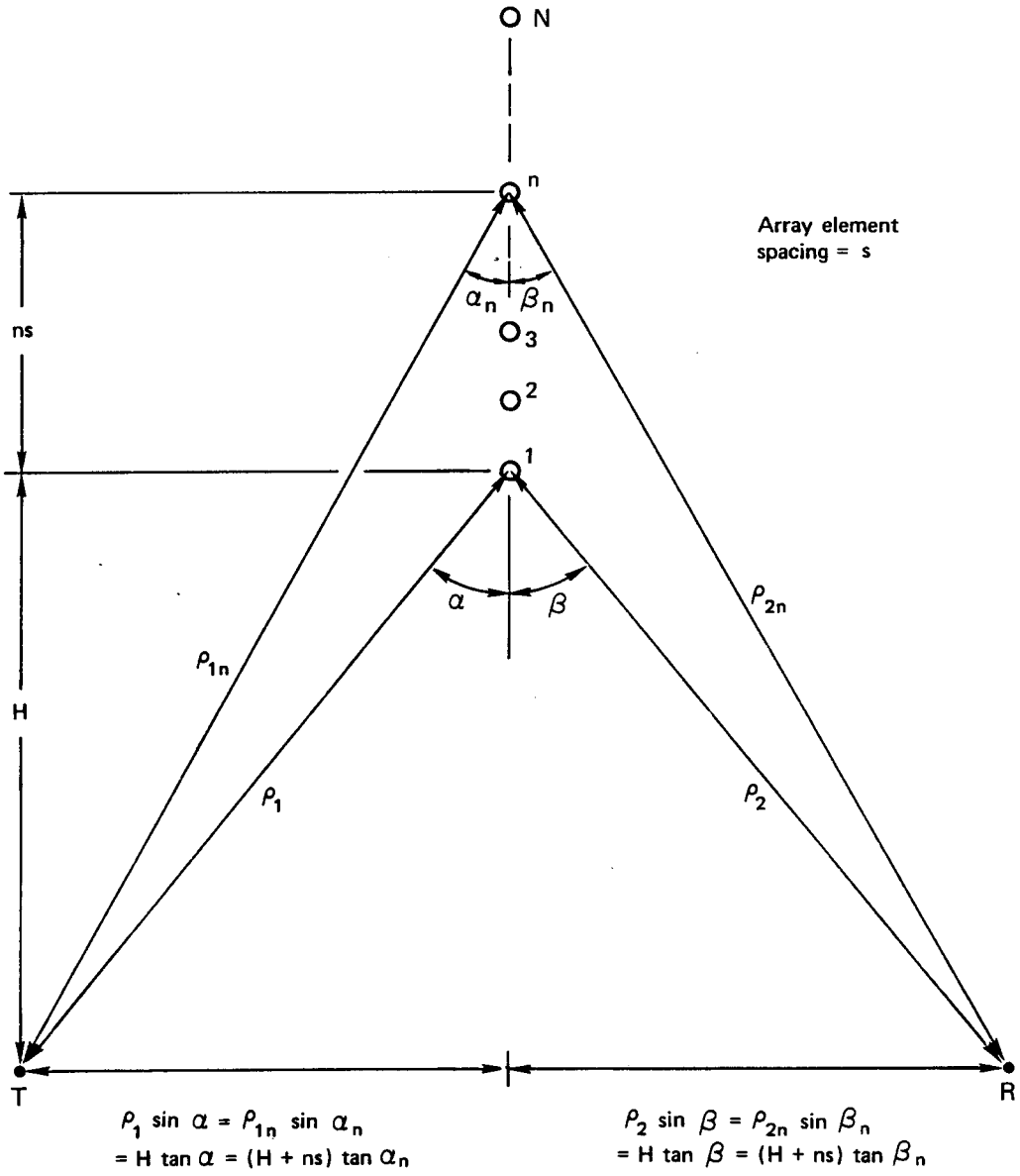


Fig. 1 — PACSAT array basic geometry

Now, defining $\rho \triangleq \rho_1 + \rho_2$ and $\rho_n \triangleq \rho_{1n} + \rho_{2n}$, the differential distance between the first and nth elements is:

$$\Delta\rho_n \triangleq \rho_n - \rho = Hns\left(\frac{1}{\rho_1} + \frac{1}{\rho_2}\right) + \frac{(ns)^2}{2}\left\{\frac{1}{\rho_1}\left[1 - \frac{H^2}{\rho_1^2}\right] + \frac{1}{\rho_2}\left[1 - \frac{H^2}{\rho_2^2}\right]\right\} . \tag{6}$$

The differential propagation time delay is obtained by dividing (6) by the propagation velocity of light, c, viz

$$\Delta\tau_n \triangleq \frac{\Delta\rho_n}{c} = n\underbrace{\left[\frac{Hs}{\rho_1 c}\right]}_{\tau_1} + \underbrace{\left[\frac{Hs}{\rho_2 c}\right]}_{\tau_2} + \underbrace{\frac{(ns)^2}{2c}\left\{\frac{1}{\rho_1}\left[1 - \frac{H^2}{\rho_1^2}\right] + \frac{1}{\rho_2}\left[1 - \frac{H^2}{\rho_2^2}\right]\right\}}_{\tau_n} . \tag{7}$$

By design, the time delay $\tau_1 + \tau_2$ is to be such that, when the array is illuminated by a frequency, $f_o$,

$$f_o(\tau_1 + \tau_2) = 1 . \tag{8}$$

Noting from Fig. 1 that $H/\rho_1 = \cos\alpha$ and $H/\rho_2 = \cos\beta$,

$$f_o(\tau_1 + \tau_2) = \frac{sf_o}{c}(\cos\alpha + \cos\beta) = 1 . \tag{9}$$

When $\alpha = \beta = 0$ (end-fire condition), $2sf_o/c = 1$, or $f_o = c/2s$. Designating this particular frequency by the symbol $f_\ell$, i.e.,

$$f_\ell = \frac{c}{2s} , \tag{10}$$

and substituting this back into (9), the fundamental frequency steering relationship for the array is obtained:

$$f_o = \frac{2f_\ell}{\cos\alpha + \cos\beta} . \tag{11}$$

The selection of $f_\ell$ is the option of the system designer; however, once it is fixed, then the inter-element spacing of the array elements, s, is established by (10).

Using the relationships (8), (10), and (11), (7) may be rewritten as:

$$\Delta\tau_n = \frac{n}{f_o} + \frac{n^2 c}{2f_\ell f_o H}\left[\frac{\cos(\alpha)\ \sin^2(\alpha/2) + \cos(\beta)\ \sin^2(\beta/2)}{\cos(\alpha) + \cos(\beta)}\right] . \quad (12)$$

The differential phase delay of the carrier at frequency $f_o = \omega_o/2\pi$ is given by $\omega_o \Delta\tau_n \triangleq \Delta\phi_n$, thus:

$$\Delta\phi_n = 2\pi n + \frac{\pi n^2 c}{f_\ell H}\left[\frac{\cos(\alpha)\ \sin^2(\alpha/2) + \cos(\beta)\ \sin^2(\beta/2)}{\cos(\alpha) + \cos(\beta)}\right] . \quad (13)$$

The second term in (13) represents the quadratic curvature of the wave front that builds along the array. Differentially between successive elements it is very small; however, when n is large, its value relative to the first element cannot be ignored for certain altitudes H (especially when H is one earth radii or less). It thus manifests itself as the near-field problem. For the sake of the ensuing discussions, it will be given the symbol $\phi_n$, i.e.,

$$\phi_n \triangleq \frac{\pi n^2 c}{f_\ell H}\left[\frac{\cos(\alpha)\ \sin^2(\alpha/2) + \cos(\beta)\ \sin^2(\beta/2)}{\cos(\alpha) + \cos(\beta)}\right] . \quad (14)$$

Equations (7) and (13), together with the connecting relationships, suggest a useful signal model for the array, shown in Fig. 2. The model* consists of a pair of tapped delay lines interconnected by phase shifters. The delay sections, $\tau_1$ and $\tau_2$, are as defined in (7), and respectively represent the inter-element arrival delay time for a plane wave incident from the angular direction $\alpha$, and the inter-element scattering delay time for a plane wave received (in the far-field) at

*Finite dimension and mutual coupling effects between the elements have been ignored.

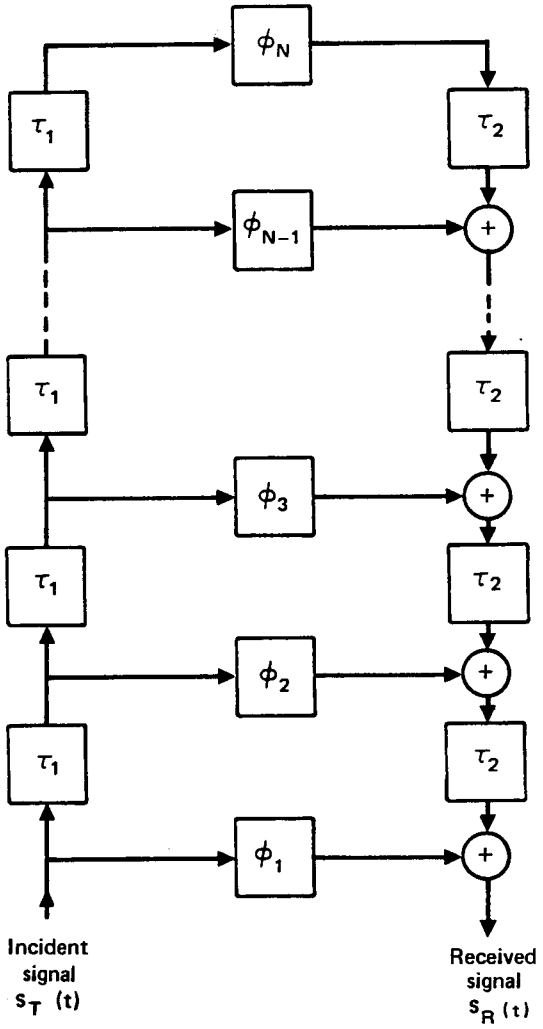


Fig. 2 — Array signal transfer function model

an angular direction $\beta$. At the carrier frequency $f_o$, $\tau_1 + \tau_2$ effectively delays the wave by one full cycle or shifts it in phase by $2\pi$. The model uses delay sections rather than phase shifters because, in general, the carrier is modulated and phase shifters alone (valid only at $f_o$) are insufficient. On the other hand, the quadratic delay components ($\tau_n$ of (7)) are extremely small and do not represent any real effect on the modulation. Therefore, it is appropriate to model the $\tau_n$ as phase shifts only of the carrier frequency, each phase shift, $\phi_n$, being given by (14).

If a signal $S_T(t) = m(t)\cos(\omega_o t)$ is input to the array model of Fig. 2, the received signal is given by:

$$S_R(t) = \sum_{n=1}^{N} m[t - (n-1)\tau] \cos[\omega_o t - \phi_n] , \qquad (15)$$

where $\tau = \tau_1 + \tau_2$. When the modulation m(t) varies slowly so that its delay, for $n \leq N$, can be ignored, then (15) simplifies to:

$$S_R(t) \cong m(t) \sum_{n=1}^{N} \cos[\omega_o t - \phi_n] . \qquad (16)$$

Finally, for an ideal array operating under far-field conditions, the $\phi_n$ are negligible ($\phi_n = 0$) and the received signal becomes:

$$S_R(t) \cong m(t) \sum_{n=1}^{N} \cos(\omega_o t) = Nm(t)\cos(\omega_o t) . \qquad (17)$$

The right-hand expression of (17) represents perfect in-phase coherent combining of the reflections from each array element.

The model of Fig. 2 with all $\phi_n = 0$ is useful for deriving certain properties of the array. The impulse response of the array for this case is easily written by inspection as:

$$h(t) = \sum_{n=1}^{N} \delta[t - (n - 1)\tau], \tag{18}$$

where $\delta(t)$ is the usual Dirac delta function. Taking the Fourier transform of (18) produces the transfer function for the array, viz.,

$$H(\omega) = F\{\delta(t)\} = \sum_{n=1}^{N} \exp[- j(n - 1)\tau\omega] \ . \tag{19}$$

Since the series in (19) is a geometrical progression, it is easily summed to yield:

$$H(\omega) = \frac{\exp[- jN\tau\omega] - 1}{\exp[- j\tau\omega] - 1} \ . \tag{20}$$

The magnitude-squared of $H(\omega)$ is calculated to be ($\omega = 2\pi f$):

$$|H(f)|^2 = \frac{\sin^2(\pi N\tau f)}{\sin^2(\pi\tau f)} \ . \tag{21}$$

Clearly, $|H(\omega)|^2$ is a periodic function of f. Since the context calls for operation of the array at a frequency in the vicinity of $1/\tau$, (21) can be rewritten in the form:

$$|H(f)|^2 = \frac{\sin^2 [\pi N\tau(f - f_o)]}{\sin^2[\pi\tau(f - f_o)]} \ , \tag{22}$$

where $f_o = 1/\tau$, and has already been given in terms of the end-fire frequency by (11).

As one example of the utility of (22), the -3 dB bandwidth of the array is calculated. When $f = f_o$, $|H(f)| = N$. Thus, it is necessary to determine the values of f for which $|H(f)| = N/\sqrt{2}$ , i.e., there exists $f_1 < f_o$ and $f_2 > f_o$ for which

$$\frac{\sin[\pi N\tau(f_o - f_1)]}{\sin[\pi\tau(f_o - f_1)]} = \frac{\sin[\pi N\tau(f_2 - f_o)]}{\sin[\pi\tau(f_2 - f_o)]} = \frac{N}{\sqrt{2}} \tag{23}$$

Letting, say, $x = \pi\tau(f_o - f_1)$, it is sufficient to solve for x in the expression

$$\frac{\sin(Nx)}{\sin(x)} = \frac{N}{\sqrt{2}} \quad . \tag{24}$$

Because the bandwidth is narrow compared to the center frequency $f_o$, x will be small ($x << \pi$), so that $\sin(x) \cong x$, and (24) can be rewritten as:

$$\frac{\sin(Nx)}{(Nx)} = \frac{1}{\sqrt{2}} \quad . \tag{25}$$

Reference to a table of sin(z)/z quickly reveals that $Nx = 1.39$. Thus, $N\pi\tau(f_o - f_1) = 1.39$, or

$$f_o - f_1 = \frac{1.39}{N\pi\tau} = \frac{1.39}{N\pi} f_o \quad . \tag{26}$$

Now, $f_o - f_1$ is one-half of the -3 dB bandwidth; therefore, the total -3 dB bandwidth is twice that given by (26), or:

$$BW(-3\ dB) = \frac{2.78}{N\pi} f_o = \frac{0.885}{N} f_o \tag{27}$$

Substituting (11) for $f_o$ in (27) yields:

$$BW(-3\ dB) = \frac{1.77\ f_\ell}{N(\cos\alpha + \cos\beta)} \tag{28}$$

This result shows that the bandwidth is inversely proportional to the length of the array, and increases as the angles to the array increase.

Further applications of the model and relationships developed in this section will be made in Sections III and IV.

## III. SIGNAL FREQUENCY ACQUISITION

The problem of frequency acquisition may be readily appreciated by resort to a typical use scenario.

An airborne command post (ABNCP) is to communicate sequentially with M MX receivers via the PACSAT in equatorial orbit. Depending upon the location of the ABNCP, the MX field, and the PACSAT, there exists a range of angles $\alpha$ and $\beta$ which encompasses all communication scenarios.

At any instant of time, the ABNCP knows the $\alpha$ and $\beta$ necessary to place a given MX receiver at the center of the PACSAT return illumination annulus. This is by virtue of a priori MX movements, computer projections of the PACSAT location, and accurate ABNCP coordinate determination. The MX receiver is also assumed to know the requisite $\beta$, however, $\alpha$ is generally unknown to the receiver because there is no realistic way to communicate this information from the ABNCP to the MX site. Thus, the receiver must expect the $\alpha$ to fall on some range of values dependent upon the immediate $\beta$ and the limits imposed upon $\alpha$ from flight range constraints on the ABNCP relative to some geographic center.

For a given $\beta$, there is a corresponding $\alpha$, which, from the receiver's viewpoint, falls on a range:

$$\alpha_1 \leq \alpha \leq \alpha_2 \ .$$

Furthermore, considering the total MX field and all useful PACSAT orbit positions (or the range of orbit positions), $\beta$ could be any angle on the range:

$$\beta_{min} \leq \beta \leq \beta_{max} \ .$$

The $\alpha$ uncertainty translates into a transmitted frequency uncertainty at the receiver. This frequency uncertainty is obtained using (11) as: $(\alpha_2 > \alpha_1)$

$$\Delta f = \left[ \frac{1}{\cos \alpha_2 + \cos \beta} - \frac{1}{\cos \alpha_1 + \cos \beta} \right] 2f_\ell \qquad (29)$$

where $f_\ell$ is the transmission frequency used for the PACSAT array end-fire condition of $\alpha = \beta = 0$. Thus, the receiver must acquire over this range of frequency uncertainty. To be realistic, the frequency acquisition should not significantly extend the time necessary to transmit the basic message from the ABNCP to the MX receiver.

The proposed solution to the frequency uncertainty and acquisition problem is to use a fixed set of selectable frequencies (at the transmitter) structured in the following manner. Each frequency corresponds to a specific $\alpha_n$ and $\beta_n$ pair. The frequencies are spaced so that for any exact $\alpha$ and $\beta$, there is a frequency $f_n$ (corresponding to $\alpha_n$ and $\beta_n$) for which the receiver is guaranteed to fall within the -3 dB* beam angle of the return radiation from the array. Stepping (by the transmitter) from one frequency to an adjacent frequency in the set causes the return beam to step in angle by one -3 dB* beamwidth. Thus, when the ABNCP determines the $\alpha$ and $\beta$ to communicate with a particular MX receiver, it selects the closest $\alpha_n$ and $\beta_n$ pair, and uses the corresponding transmission frequency, $f_n$.

The receiver is assumed to know $\beta$ (by virtue of computer prediction, or direct measurement using self-illumination by a signal transmitted to the array from the receiving site). However, only the nominal $\alpha$ (ABNCP geographic center) is known to the receiver, and there is an uncertainty range, $\alpha_1$ to $\alpha_2$. Since the receiver knows the frequency set and the $\beta_n$ used by the transmitter, it need then only search over the candidate $f_n$ corresponding to the $\alpha_n$ values that fall within the uncertainty range.

To accomplish the frequency search, it is postulated that the receiver will use an $N_f$ channel frequency-selective energy detector. Each channel is set to an expected frequency, and has bandwidth sufficient to encompass all frequency uncertainty. (The bandwidth

*Or perhaps, in order to allow for some margin, the -2 dB beamwidth is more practical.

will be found to be considerably less than the interfrequency spacing.) The integration period and detection threshold are selected to give a high detection probability (say, $P_D = 0.999$) when a signal is present in one of the channels, and a very low false alarm probability (say, $P_{FA} = 10^{-14}$) when no signal is being received.

This, then, is the broad concept for frequency acquisition. It now suffices to explore some of the details, and to conclude with a numerical example to illustrate the probable size of the system.

To begin, the sensitivity of the return beamwidth as a function of $\alpha$ and $\beta$ is derived. The array illumination frequency, $f_o$, is given by (11) for a specified $\alpha$ and $\beta$. It should be recalled that when (11) is satisfied, the inter-element propagation times for a plane wave arriving from angular direction $\alpha$, and culminating in a far-field plane wave being received in the angular direction $\beta$, is exactly one cycle, or a $2\pi$ phase delay of $f_o$. Now, if the receiver is not located exactly at the angle $\beta$, but rather at an angle $\beta + \Delta\beta$, the phase shift between the individual returns from each element will no longer be exactly $2\pi$, and a reduced resultant combined amplitude will be obtained. In fact, for certain $\Delta\beta$, nulls (no resultant signal) are manifest.

The beamwidth may be derived by starting with the relationship (obtained from the definition of $\tau_2$ in (7), plus (10) and $\cos\beta = H/\rho_2$):

$$\cos\beta = 2f_\ell\tau_2 \ . \tag{30}$$

By deduction,

$$\cos(\beta + \Delta\beta) = 2f_\ell(\tau_2 - \Delta\tau_2) = \cos\beta - 2f_\ell\Delta\tau_2 \ , \tag{31}$$

and solving for $\Delta\beta$ yields:

$$\Delta\beta = \cos^{-1}\left[\cos\beta - 2f_\ell\Delta\tau_2\right] - \beta \ . \tag{32}$$

If the beamwidth is defined by $\delta\beta \triangleq 2\Delta\beta$, then:

$$\delta\beta = 2 \cos^{-1} [\cos \beta - 2f_{\ell}\Delta\tau_2] - 2\beta \quad . \tag{33}$$

It now remains to derive $\Delta\tau_2$. From the array model of Fig. 2, with the $\phi_n$'s = 0 and $\tau_2$ replaced by $\tau_2 + \Delta\tau_2$, the received signal is written as:

$$S_R(t) = \sum_{n=1}^{N} \cos[\omega_o t + n\omega_o(\tau_1 + \tau_2 + \Delta\tau)] \quad . \tag{34}$$

Recalling that, by design, $\omega_o(\tau_1 + \tau_2) = 2\pi$, (34) reduces to:

$$\begin{aligned} S_R(t) &= \sum_{n=1}^{N} \cos[\omega_o t + n\omega_o\Delta\tau_2] \\ &= \cos \omega_o t \sum_{n=1}^{N} \cos(n\omega_o\Delta\tau_2) \\ &\quad - \sin \omega_o t \sum_{n=1}^{N} \sin(n\omega_o\Delta\tau_2) \\ &= A_c \cos \omega_o t - A_s \sin \omega_o t \quad . \end{aligned} \tag{35}$$

Now, when $\Delta\tau_2 = 0$, $A_c = N$, and $A_s = 0$. Thus, the condition for which

$$\sqrt{A_c^2 + A_s^2} = \frac{N}{\sqrt{2}} \tag{36}$$

must be established. Summing the series representing $A_c$ and $A_s$, it may be readily shown that:

$$\sqrt{A_c^2 + A_s^2} = N \frac{\sin\left(\frac{N\omega_o \Delta\tau_2}{2}\right)}{\left(\frac{N\omega_o \Delta\tau_2}{2}\right)} \quad . \tag{37}$$

Equating (36) and (37), and solving for $\Delta\tau_2$ gives

$$\Delta\tau_2 = \frac{2.78}{N\omega_o} \quad . \tag{38}$$

Taking this result, together with (11) and (33), produces the final result for the beamwidth, viz.,

$$\delta\beta = 2 \cos^{-1}\left[\cos\beta - \frac{1.39}{\pi N}(\cos\alpha + \cos\beta)\right] - 2\beta \quad . \tag{39}$$

A study of (39) discloses that $\delta\beta$ is maximum for $\alpha = \beta = 0$ (end-fire) and decreases for increasing $\alpha$ and $\beta$. Since for the PACSAT scenario the end-fire condition does not usually occur, a more utilitarian approximation to (39) may be derived. When $\beta >> \Delta\beta$, (31) may be written approximately as:

$$\cos\beta - \Delta\beta \sin\beta \cong \cos\beta - 2f_\ell \Delta\tau_2 \ , \tag{40}$$

or

$$\Delta\beta = \frac{2f_\ell \Delta\tau_2}{\sin\beta} \quad . \tag{41}$$

Using (11) and (38) together with the definition for $\delta\beta$, the approximate and simplified result is obtained as:

$$\delta\beta \cong \frac{2.78}{\pi N}\left[\frac{\cos\alpha + \cos\beta}{\sin\beta}\right] \ , \ \beta >> \delta\beta \ , \tag{42}$$

(thus verifying Eq. (10) of [2]).

Recalling from the earlier discussion that steering the beam by means of a discrete set of transmitter frequencies is the goal, it is now of interest to determine the spacing and number of frequencies. A step from one frequency to the next will be assumed to step the beam in angle by $\delta\beta$. From (11),

$$f_o + \delta f = \frac{2f_\ell}{\cos\alpha + \cos(\beta + \delta\beta)} \tag{43}$$

$$\cong \frac{2f_\ell}{\cos\alpha + \cos\beta - \delta\beta \sin\beta} \quad . \tag{44}$$

Using (42) to substitute for $\delta\beta \sin\beta$, and simplifying, the approximate result becomes:

$$\delta f \cong \frac{2.78}{\pi N} \left[\frac{2f_\ell}{\cos\alpha + \cos\beta}\right] . \tag{45}$$

Again, recalling that the transmitter frequency adjustment range, needed to place the receiver within the -3 dB beamwidth, is $\Delta f$ given by (29), the number of discrete frequencies $N_f$ required becomes:

$$N_f = \frac{\Delta f}{\delta f} = \frac{\pi N}{2.78} (\cos\alpha + \cos\beta) \left[\frac{1}{\cos\alpha_2 + \cos\beta} - \frac{1}{\cos\alpha_1 + \cos\beta}\right] . \tag{46}$$

An example at this juncture will serve to illustrate the results of Eqs. (45) and (46). A satellite 1500 meters in length, designed to operate at an end-fire frequency of 8 GHz, will have N = 80,001 elements. For a one-earth-radius equatorial orbit altitude, typical $\alpha$ and $\beta$ values are $\alpha = 22°$ and $\beta = 35°$ (using the ABNCP and MX scenario). Assuming $\alpha_1 = 20°$ and $\alpha_2 = 24°$, the frequency set frequency spacing is found to be $\delta f = 101.3$ kHz, and the number of frequencies is calculated as $N_f = 1355$.

Attention is now turned to the means by which the MX receiver may be brought to a message receiving state.

The frequency acquisition process by the MX receiver consists of two steps: (a) detection of which frequency the transmitter is using and (b) phase-locking on the detected frequency.

Figure 3 shows a configuration for the frequency detector.* A channel is provided for each of the candidate frequencies, and each channel is functionally identical.

The accuracy of any received frequency, relative to its theoretical static-condition (time-instant) value, depends on the transmitter and receiver frequency stabilities and baseline accuracies, as well as the degree of doppler compensation at the transmitter. Generally, the input bandpass filter (BPF) to each channel of the frequency detector has a bandwidth, W, with property

$$W << \delta f, \tag{47}$$

as W need only be sufficient to accommodate the frequency uncertainty. Threshold TH is selected to obtain the desired false-alarm probability ($P_{FA}$) in the absence of a signal within a channel, and the required detection probability ($P_D$) when a signal is present. For the absence of signal, all $\mu$ outputs take on value -1, and when a signal is present in a channel, that $\mu$ output has value +1.

The integration time, T, is the dependent quantity, and is related to the other governing parameters by the relationship [4]:

$$T = Wd^2/(C/N_o)^2 , \tag{48}$$

where

$$d = Q^{-1}(P_{FA}) - Q^{-1}(P_D), \tag{49}$$

and $C/N_o$ = the received signal-to-noise spectral density power ratio.

$Q^{-1}(\ )$ is the inverse normal cumulative distribution function.

For a practical acquisition/detection procedure, an overhead of 3T seconds should be allowed for detection. T seconds are needed

*The appendix investigates an alternate approach that is simpler to implement but requires significantly increased decision time compared with the proposed configuration.

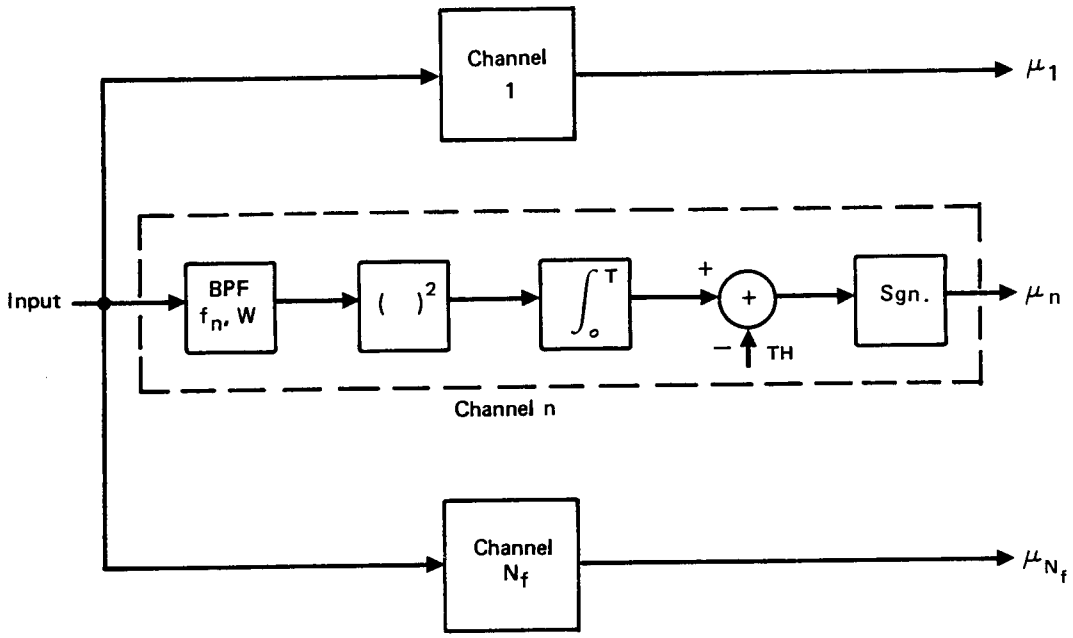


Fig. 3 — Functional frequency detector

for detection, T seconds for detection confirmation (it is assumed that two successive $\mu = 1$ conditions from the same channel are necessary to proceed to the next step), and T seconds for lack of signal onset epoch synchronization.

Once detection has been accomplished, a separate Costas-loop type receiver [5] is frequency programmed to the nominal channel frequency. This loop must then acquire the "carrier" from the range of frequency uncertainty. (The word carrier is placed in quotation marks because the received signal is assumed to be of a suppressed carrier form, and the Costas-loop regenerates a double-frequency carrier through the inherent squaring process.) Generally, it may be assumed that the frequency uncertainty will be greater than the data (or symbol) rate that modulates the carrier. As a result, Costas-loop false lock at frequency offsets of multiples of one-half of the data rate may be expected. To preclude such, it is expedient for the transmitter to remove all data modulation and transmit an unmodulated carrier during both the frequency detection and Costas-loop acquisition phases of the reception process. Thus, unmodulated carrier is transmitted by the ABNCP for a prescribed period to be defined subsequently.

The Costas loop may be acquired using one of two basic approaches [6]: (a) self-pull-in and (b) frequency sweeping. The former is the simplest to implement as nothing is required outside of the loop itself. However, the price paid is generally a moderate pull-in time. On the other hand, the sweep approach results in relatively rapid acquisition, but at increased complexity due to the addition of sweep-related circuits. The maximum frequency uncertainty is equal to one-half of the frequency detector channel bandwidth, i.e., $f_{acq} = W/2$. For a self-pull-in Costas-loop operating at a high loop SNR (say, 15 dB), the necessary conditions are (the loop damping factor is taken as unity):

$$K \geq 1.25\ (\pi W)^2/(2B_L) \tag{50}$$

and

$$T_{acq} = 1.95\ (\pi W)^2/(2B_L)^3 = 1.56K/(2B_L)^2\ , \tag{51}$$

where K is the open-loop gain and $2B_L$ is the loop two-sided noise bandwidth in Hz.

For the frequency sweeping scheme, the sweep rate $f_{sw}$ is given by:

$$f_{sw} \leq 0.112 \ (2B_L)^2 \text{ Hz/sec.} \tag{52}$$

Equality results in a 0.9 probability of acquisition.

If the sweep profile is taken as a linear frequency sweep from one edge of the band W to the other, and then a return to the center of the band (i.e., removal of the sweep for the nominal frequency value), the acquisition time is given by:

$$T_{acq} = 1.5 \ W/f_{sw} \ . \tag{53}$$

To obtain a measure of the relative time involved for both acquisition methods, the ratio of (51) to (53) is taken for the maximum allowable sweep rate [equality in (52)], thus:

$$\frac{T_{acq} \ (\text{self-pull-in})}{T_{acq} \ (\text{swept loop})} = \frac{1.44 \ W}{2B_L} \ . \tag{54}$$

Clearly, whenever W is significantly larger than $2B_L$, the swept acquisition approach is essential to acquisition time minimization. For the PACSAT applications under consideration, W is expected to be at least an order of magnitude larger than $2B_L$. Swept frequency acquisition will therefore be assumed.

To close this section, consideration is given to the total time required by the ABNCP to communicate an $N_m$ bit message to a selected MX site. The total time is that necessary for frequency detection, frequency acquisition, symbol synchronization, and the actual message content. Frequency detection and acquisition time have already been discussed.

Symbol synchronization and message times are measured in bits. If an alternating +1 and -1 pattern is used to rapidly establish symbol synchronization by means of a digital transition tracking loop (DTTL) synchronizer, the maximum time necessary to acquire is about 120 symbol periods. With a symbol rate of $R_S$ symbols per second, then $120/R_S$ is the absolute time necessary to acquire symbol synchronization.

Figure 4 shows the time components necessary to transmit and receive one total message. In order to virtually guarantee the Costas-loop swept frequency acquisition, the maximum allowable sweep rate [equality in Eq. (52)] has been backed off by 20 percent.

At this point, a numerical example again illuminates the reality of the total communication time. The following assumed parameter values are considered typical of the ABNCP/MX scenario.

$$
\begin{aligned}
N_M &= 400 \text{ bits} \\
R_S &= 1000 \text{ symbols/sec} \\
C/N_o &= 40 \text{ dB - Hz} \\
W &= 4 \text{ KHz} \\
2B_L &= 250 \text{ Hz} \\
P_D &= 0.999 \\
P_{FA} &= 10^{-14}
\end{aligned}
\Bigg\} \quad d = 10.75
$$

With reference to Fig. 4, the total time is calculated to be 1.634 sec, composed of the following components:

Frequency detection time = 0.014 sec
Costas-loop acquisition time = 1.1 sec
Symbol synchronization time = 0.12 sec
Message time = 0.4 sec.

It should be noted that the largest component is the Costas-loop acquisition time. Practically, this can only be made smaller by taking steps to reduce frequency uncertainty.

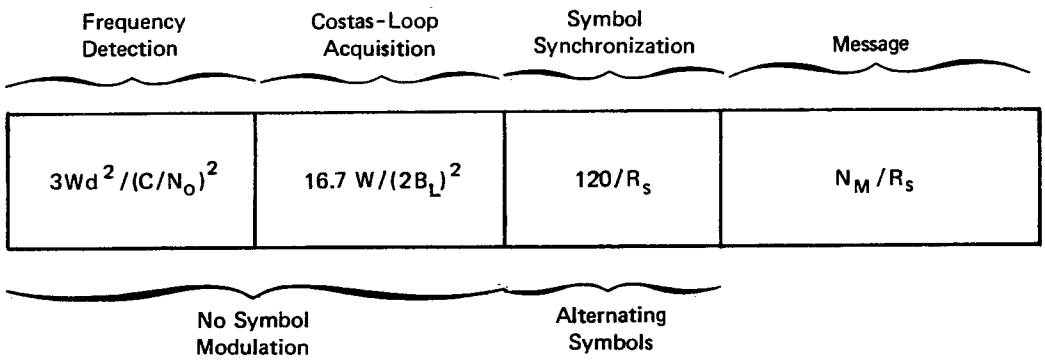


Fig. 4 — Total message time components

As a final observation, it is seen from the above that the smallest component of the total communication time is that for frequency detection. At a small expansion in total time--from 1.634 sec to 1.76 sec--the frequency detection time is increased by a factor of 10. Through this modest increase, an effective hardware savings is obtained in the number of physical detection channels required by the frequency detector from 1355 channels (see earlier example) to 49 channels. Frequency detection is then effected by hopping the 49 channels over the total set of 1355 frequencies.

## IV. PROCESSING FOR NEAR-FIELD PHASING ERROR

When the PACSAT is in low earth orbit (one earth radius or less), and the array is sufficiently long (say, 1500 meters), the quadratic curvature of the wavefront that builds across the array becomes significant to the extent that the receiver is not in the far-field of the reflected wave. Thus, unless some means is provided to correct the incremental misphasing of the return waves from each element of the array, an effective loss of signal power results from the quadratic terms.

A second source of phasing error results from a mechanically non-ideal array. Because of various forces acting on the array, the individual elements are expected to be displaced (with constraints) from their ideal locations, as shown in Fig. 5. Although these displacements will be small, they could represent equivalent phase errors of many degrees. Furthermore, the displacements must be treated as random (although they will be correlated over short segments of the array) and time varying.

Before proceeding with the development of a solution to the phasing problem, an example of the magnitude of the near-field loss is illustrative. Equation (14) is rewritten in the form:

$$\phi_n = \varepsilon n^2 \tag{55}$$

with

$$\varepsilon \triangleq \frac{\pi c}{f_\ell H}\left[\frac{\cos(\alpha)\,\sin^2(\alpha/2) + \cos(\beta)\,\sin^2(\beta/2)}{\cos(\alpha) + \cos(\beta)}\right] . \tag{56}$$

The coefficient $\varepsilon$ increases with increasing $\alpha$ and $\beta$. For the sake of the example, $\alpha$ and $\beta$ are both taken to be 30°. Additionally, $H$ = 1 earth radius (6378 km) and $f_\ell$ = 8 GHz. Calculation of $\varepsilon$ using (56) gives $\varepsilon = 1.237 \times 10^{-9}$ radian. The effective signal loss is now calculated using the array center element as reference for the nominal $\alpha$ and $\beta$ angles, yielding:

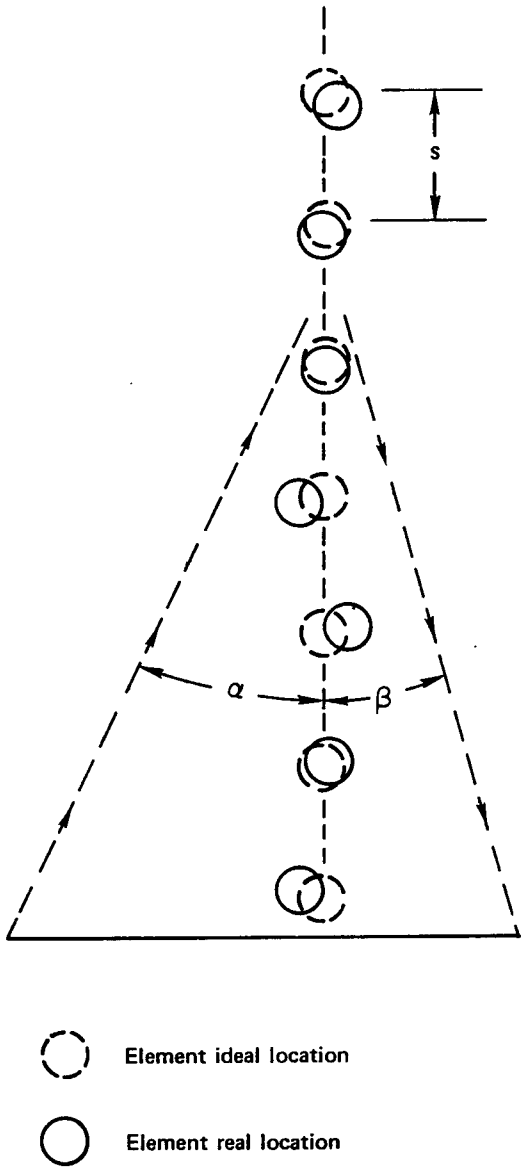


Fig. 5 — Nonideal array having displaced elements

$$\text{Loss} = \frac{1 + 2\sum_{n=1}^{(N-1)/2} \cos(\varepsilon n^2)}{N} , \qquad (57)$$

where N is the number of array elements. Taking N = 80001 (1500 meter array length), the loss obtained from (57) is -3.4 dB. Clearly, this loss is of sufficient magnitude to justify the use of a corrective procedure.

The preceding example assumed continuous wave (cw) illumination of the array. In order to simply develop the near-field processing concept, assume that in place of a continuous RF wave a pulsed RF wave is used, with a pulse width equal to the propagation delay time $\tau_1 + \tau_2$ [given by (9)], and a pulse repetition frequency (PRF) equal to the inverse of the propagation delay for the entire array, i.e.,

$$\text{PRF} = [(N-1)\ (\tau_1 + \tau_2)]^{-1} . \qquad (58)$$

With such pulsed illumination, the received wave is composed of a series of phase-disjoint sequential reflections from the individual elements, as illustrated in Fig. 6. It is seen that the received signal is thus composed of segmented terms, each with increasing phase error in accord with Eq. (14).

Figure 7 shows a conceptual near-field processing receiver that corrects for the $\phi_n$ components. A voltage-controlled phase shifter is used to sequentially shift each received wave segment by $-\phi_n + \phi_1$, so that at the output a continuous phase signal (with reference phase $\phi_1$) is obtained. Thus, all of the deterministic phase error is effectively removed. (Note: random phase errors cannot be processed away by this simple approach because they are not known a priori at the receiver.)

Although the foregoing approach to solving the near-field problem works in principle, it is far from practical. Consider the following requirements based upon the previously cited system parameters ($\alpha = \beta = 30°$, N = 80001, S = 1.875 cm). The pulse width is calculated to

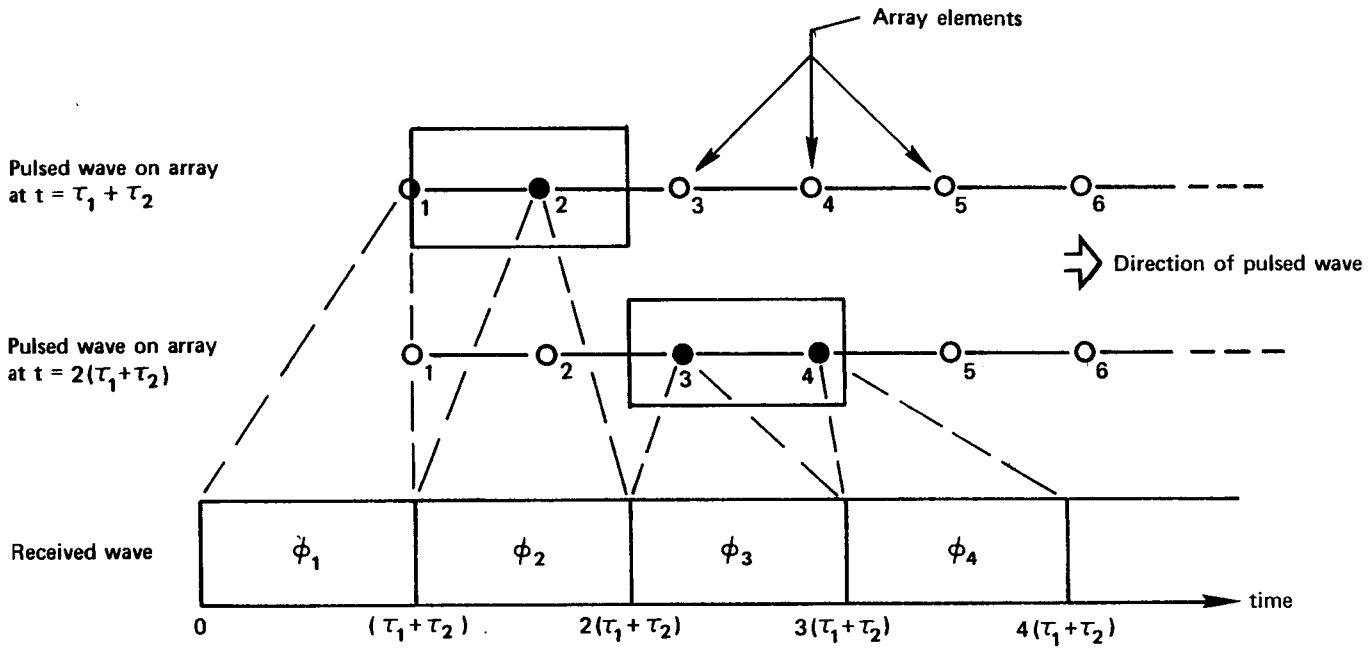


Fig. 6 — Pulsed RF wave propagation states and received wave structure

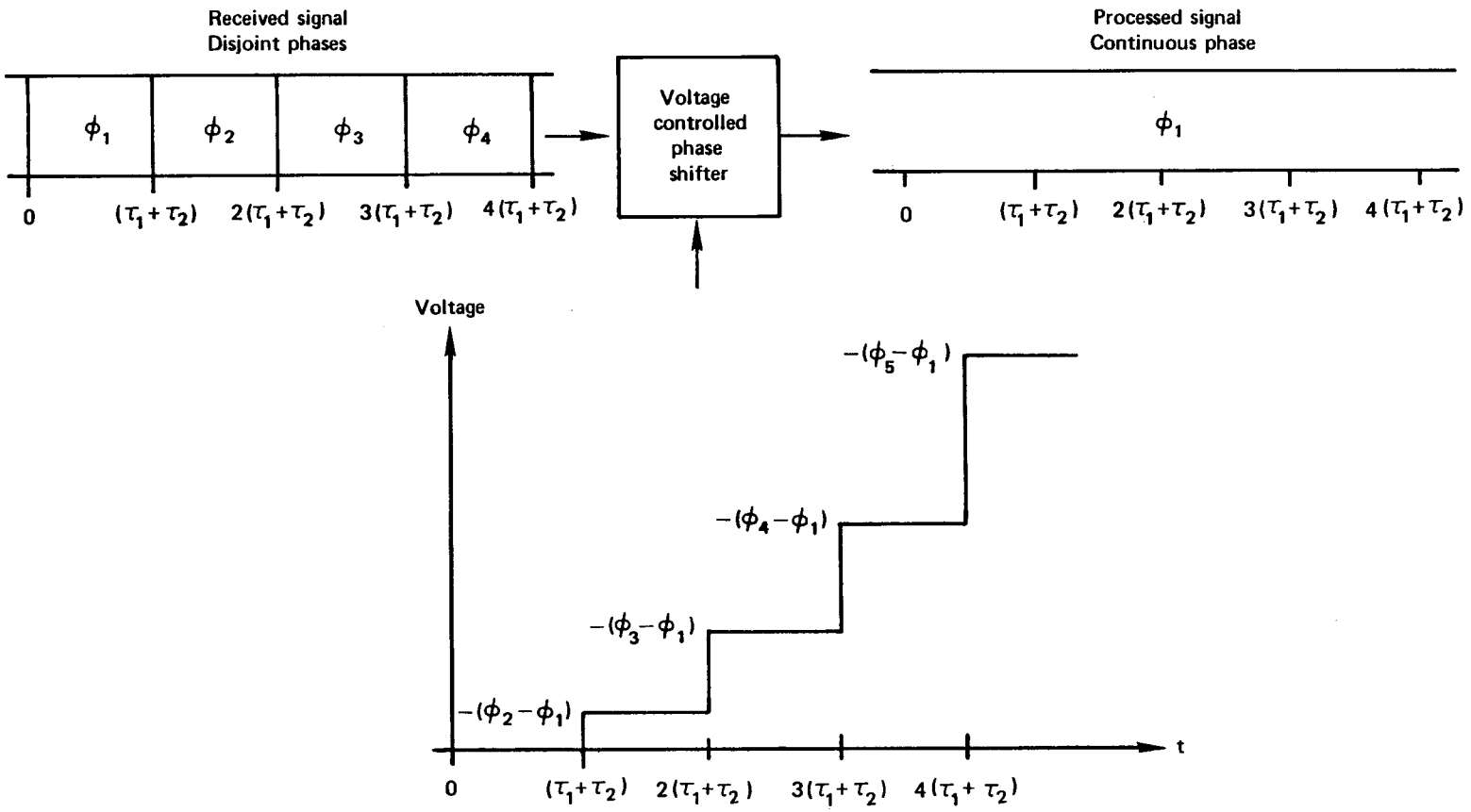


Fig. 7 — Conceptual near-field processing receiver

be $\tau_1 + \tau_2 = 0.1$ ns, and PRF = 115.5 KHz. Also, if each pulse is to supply the same received energy as that of the cw signal having power $P_{cw}$, then the pulse power is given by:

$$P_{pulse} = (N - 1)P_{cw} . \tag{59}$$

Typical communication link calculations show that $P_{cw}$ should be on the order of 100 W. Equation (59) then requires that $P_{pulse} = 8$ MW! Clearly, the required pulse width and power, together with the implied switching and processing speeds, render the pulsed wave concept unachievable.

Before proceeding with a description of a practical near-field correction method, the requirement for correction is reevaluated. The value of $\varepsilon = 1.237 \times 10^{-9}$ radian is very small, so small, in fact, that correction of phase on an element-to-element basis is unwarranted. Therefore, it is reasonable to view the total array as a spatial series of subarrays, each having N′ elements. The combined returns from each subarray are then accepted with some loss, and near-field phase correction is made only to the mean phase of the return from each individual subarray. In order to assess how large a subarray may be, consider the following table of near-field dephasing losses.

| N′ | Dephasing Loss |
|---|---|
| 500 | -0.02 dB |
| 1000 | -0.04 dB |
| 2000 | -0.07 dB |
| 4000 | -0.16 dB |

A loss of less than -0.2 dB is judged to be quite acceptable. Thus, N′ = 4000 is selected, dividing the total array in 20 subarrays. (Actually, it is the random phase components arising from element displacements that are likely to limit the size of N′. However, since the true magnitude of such displacements remains to be evaluated, N′ = 4000 is assumed for the ensuing development.)

Returning, now, to the pulsed wave concept, assume that a pulse is transmitted whose width on the array spans 4000 elements. (Such a pulse would have a very practical width of 0.4 μs.) Unlike the very narrow pulse whose return from each element is time separable at the receiver (Figs. 6 and 7), the return from 4000 simultaneously illuminated elements produces time overlapping signals with respect to the specified subarrays. Thus, discrimination between the subarrays on the basis of simple time gating is not possible. Theoretically, a means is needed to illuminate a 4000-element segment of the array, and then instantly hop the illumination to the next 4000-element segment, etc. One way of accomplishing such illumination could be to use a transmitting aperture of sufficient size to cause a beamwidth so narrow that only 4000 elements are subtended at a time. It should be apparent that this approach is more unworkable than the narrow pulse method because it would require an aperture larger than the array itself.

The practical solution is based on the use of the correlation properties of pseudo-noise (PN) codes [5]. Rather than transmitting a pulse whose width covers 4000 elements, a continuous wave carrier is biphase modulated by a PN code whose chip period spans the 4000 elements. For the previously cited parameters, a PN chip rate of 2.5 MHz is required. Furthermore, because modulation of a continous wave is involved, $P_{pulse} = P_{cw}$. Thus, the pulse width and power specifications are well within attainable limits.

Consider a signal of the form:

$$s_T(t) = PN(t) \cos[\omega_o t] \ , \tag{60}$$

input to the array model of Fig. 2. From Eq. (15), the received signal will be:

$$s_R(t) = \sum_{n=0}^{N-1} PN(t - n\tau) \cos[\omega_o t + \phi_{n+1}] \ , \tag{61}$$

where $\tau = \tau_1 + \tau_2$, and the PN chip period is $N'\tau$. If the received signal given by (61) is correlated at the receiver with PN(t), the

resulting correlation function obtained is (the average being taken only on the PN components):

$$r_o(n\tau;\ t) = \langle s_R(t)\ PN(t)\rangle$$

$$= \sum_{n=0}^{N-1} \langle PN(t)\ PN(t - n\tau)\rangle \cos[\omega_o t + \phi_{n+1}]$$

$$= \sum_{n=0}^{N-1} r_{PN}(n\tau)\ \cos[\omega_o t + \phi_{n+1}] \ . \qquad (62)$$

The term $r_{PN}(n\tau)$ is the autocorrelation of the PN code,* and is shown in Fig. 8. In effect, this function weights the cosine terms of Eq. (62) so that Eq. (62) may be written as:

$$r_o(n\tau;\ t) = \sum_{n=0}^{N'} \left(1 - \frac{n}{N'}\right) \cos[\omega_o t + \phi_{n+1}] \ . \qquad (63)$$

It is readily seen that (63) involves the returns from only the first $N' = 4000$ elements.

Next, correlate (61) with $PN(t - N'\tau)$. The result becomes:

$$r_1(n\tau;\ t) = \sum_{n=0}^{N-1} r_{PN(N'\tau)}\ (n\tau)\ \cos[\omega_o t + \phi_{n+1}] \ . \qquad (64)$$

The term $r_{PN(N'\tau)}\ (n\tau)$ is drawn in Fig. 9, where $r_{PN}\ (n\tau)$ is also shown for comparison. By inspection of Fig. 9, (64) is written as:

$$r_1(n\tau;\ t) = \sum_{n=0}^{N'} \frac{n}{N'} \cos[\omega_o t + \phi_{n+1}]$$

$$+ \sum_{n=N'}^{2N'} 2\left(1 - \frac{n}{2N'}\right) \cos[\omega_o t + \phi_{n+1}] \ . \qquad (65)$$

---

*The autocorrelation has been normalized to its maximum value.

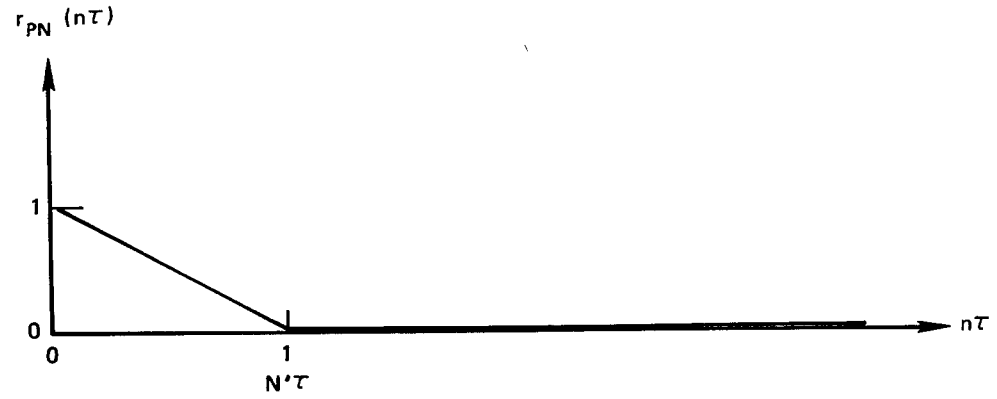


Fig. 8 — PN code autocorrelation function

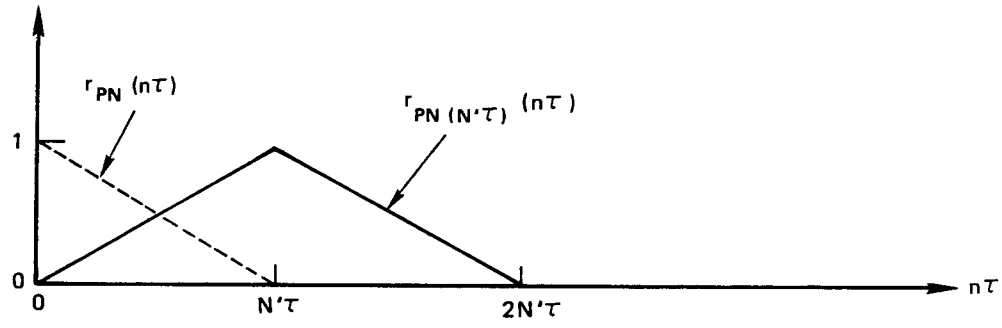


Fig. 9 — Correlation function between PN (t) and PN ($t-N'\tau$)

It can be seen that (65) involves the returns from the first $2N' = 8000$ elements. Note, however, that the weightings over the first $N'$ returns are just the opposite from the weightings in Eq. (63).

In a similar fashion, additional correlations are made at multiples of $N'\tau$. Each additional correlation will produce a weighting triangle like that of Fig. 9, but displaced in $N\tau$ by the multiple of $N'\tau$. Thus, each correlator (except for the two end correlations) produces a weighted sum of the dephased returns from $2N'$ elements. Because the adjacent correlation functions overlap, the correlator outputs are not independent since $N'$ elements are in common. Nevertheless, sufficient discrimination is obtained so that the output of any given correlator can be represented in the form:

$$s_k(t) = A_k \cos[\omega_o t - \psi_k] \ , \qquad (66)$$

$$k = 0,1,2, \cdots, \frac{N}{N'} \ .$$

The amplitude, $A_k$, and phase, $\psi_k$, are both deterministic functions of the quadratic phase terms, $\phi_n$, and the weighting triangle. Thus, $\psi_k$ may be corrected relative to a specified reference. Figure 10 illustrates a functional PN correlation processing receiver that performs all of the above indicated operations. The bandpass filters (BPF) effectively perform the correlation averaging or weighting. Each channel is phase corrected to the value $\psi_1$.

A practical PACSAT processing receiver must perform several functions. In addition to making the needed near-field phase corrections, it must also phase-lock to the carrier and demodulate the message data placed on the carrier. (Data are assumed to be biphase modulated onto the cw carrier in a manner identical to that of the PN modulation.) Figure 11 shows a practical method for accomplishing all three functions. Only a single channel of the $(N + 1)/N'$ channels is depicted in detail, with the interfaces to all other channels as indicated.

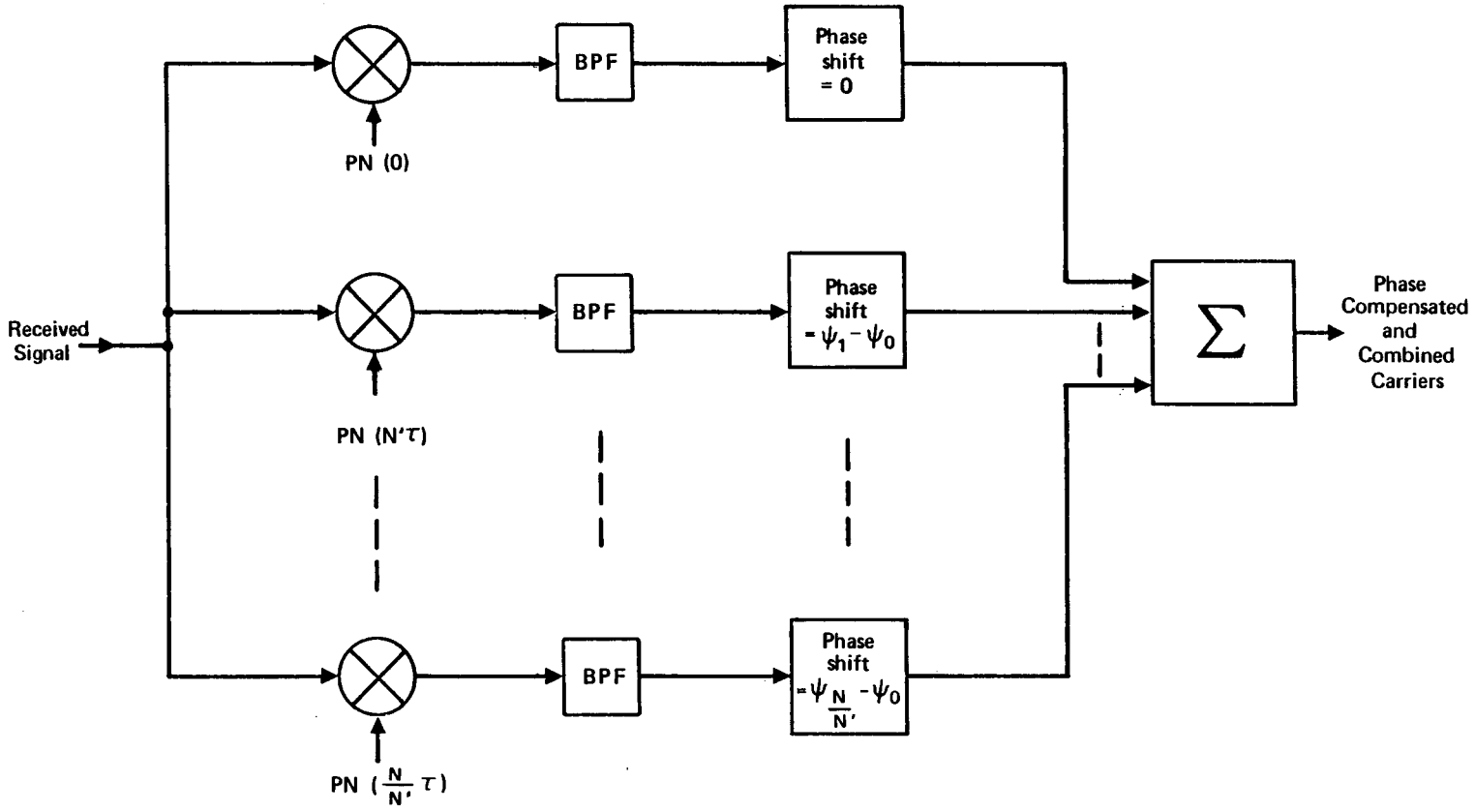


Fig. 10 — Functional PN correlation processing receiver

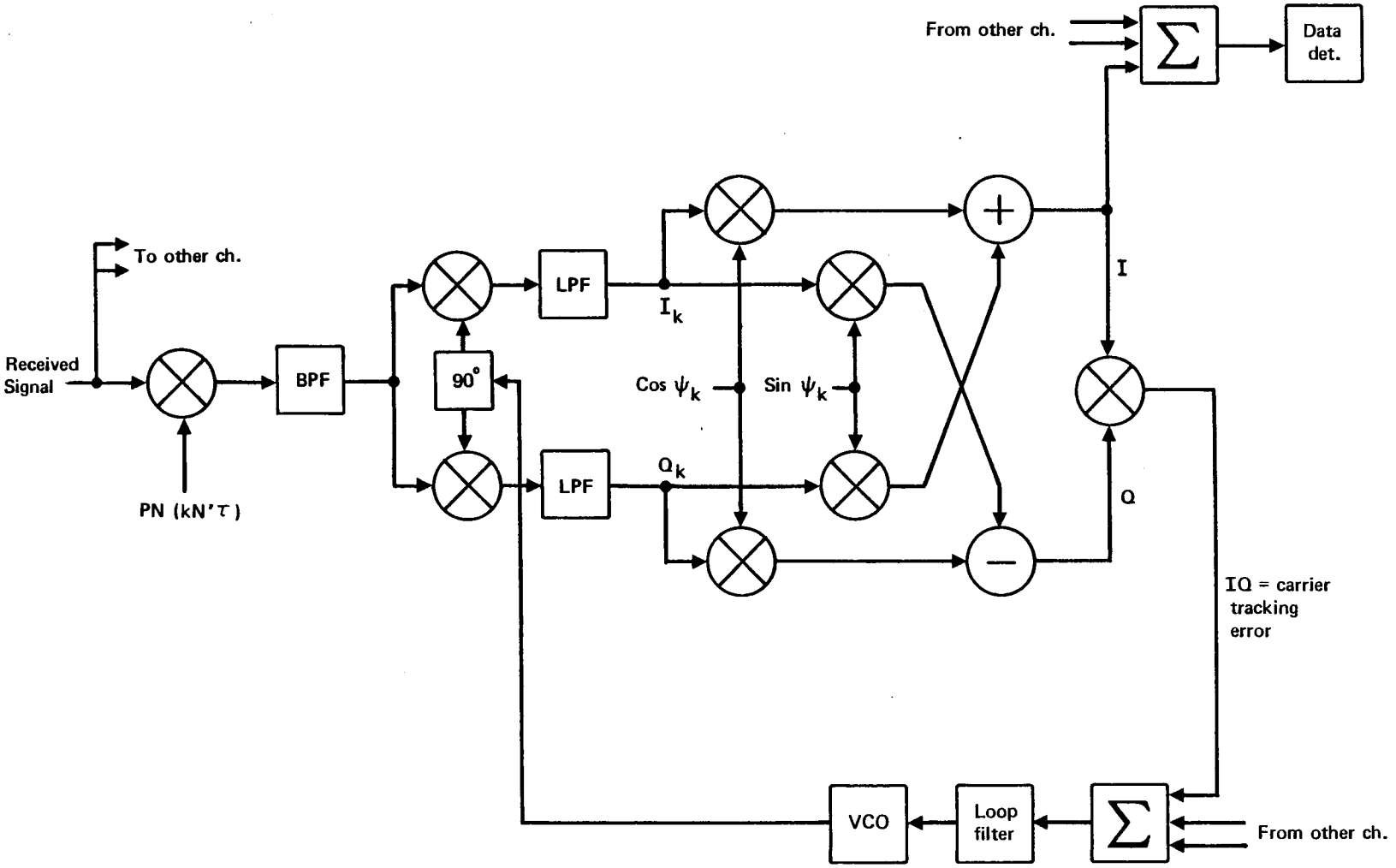


Fig. 11 — Practical PACSAT processing receiver

PN correlation and averaging takes place in a combination of bandpass and lowpass filtering. Following the PN correlator, the signal is demodulated in the usual inphase ($I_k$) and quadrature phase ($Q_k$) manner. Subsequent to demodulation and lowpass filtering (LPF), phase correction is implemented by means of arithmetic operations on the $I_k$ and $Q_k$ components, as shown in Fig. 11. The phase correction involves the functions:

$$I = I_k \cos \psi_k + Q_k \sin \psi_k \tag{67}$$

and

$$Q = I_k \sin \psi_k - Q_k \cos \psi_k \quad . \tag{68}$$

Note that no physical phase shifters are used; the processing will most likely be carried out using digital circuits.

Carrier coherence is obtained by means of a Costas-loop configuration. The product IQ forms the carrier tracking error function, which is summed with similar IQ terms from the other channels. The composite tracking error is then filtered and applied to the input of a voltage controlled oscillator (VCO). Output of the VCO is phase-split into quadrature components and applied to the $I_k$ and $Q_k$ demodulators, thus closing the tracking loop.

Finally, the I terms from each channel are summed to form the demodulated data component, which is subsequently symbol synchronized and detected.

## V. CONCLUSIONS AND FURTHER WORK

This Note has examined the problems and some possible solutions to the signal acquisition and receiver processing of PACSAT relayed messages. Although much groundwork has been laid, more effort is needed to fully analyze and develop the concepts. In particular, more work should be accomplished in the following areas.

1. Using the PN method of subarray signal discrimination, a complete analysis of the theoretical gains obtainable as a function of subarray size and PN correlation dependence is needed.
2. Although the likelihood of random phase errors due to array element displacement has been mentioned, no specific solution for possible correction has been proposed. Thus, an investigation of the means and degree to which the random components may be estimated and corrected is required.
3. A complete functional development of a total processing receiver should be undertaken. Aspects to be included are:
    a. Means for PN code synchronization.
    b. Frequency acquisition/detection details.
    c. Automatic gain control.
    d. Digital processing algorithms.
    e. Implementation risk and cost estimates.

## REFERENCES


1. Yater, J. C., "Signal Relay Systems Using Large Space Arrays," *IEEE Transactions on Communications*, Vol. COM-20, No. 6, December 1972, pp. 1108-1121.

2. Edson, W. A., et al., *Passive Space Communication Array (PACSAT)*, Stanford Research Institute, Final Report, Part One, prepared for Defense Communication Agency, Contract DCA100-76-C-0056, October 1976.

3. Bedrosian, E., *Communication Aspects of the Application of PACSAT to MX Command and Control*, Rand Note in preparation.

4. Woodring, D., and J. Edell, *Detectability Calculation Techniques*, Naval Research Laboratory Report, SCTN 1977-1, September 1, 1977.

5. Lindsey, W. C., and M. K. Simon, *Telecommunication Systems Engineering*, Prentice-Hall, Inc., 1973.

6. Blanchard, A., *Phase-Locked Loops: Application to Coherent Receiver Design*, John Wiley & Sons, 1976.

Appendix

## AN EFFICIENT CIRCUIT FOR FINDING A CARRIER IN A WIDE BANDWIDTH*

I. S. Reed

### INTRODUCTION

Some time ago the author of this appendix introduced a circuit for detecting a sine wave of unknown frequency in a wide bandwidth [1,2,3]. The circuit was called an autocovariance filter. The detection criterion associated with this circuit has been termed semicoherent detection.

The purpose of this appendix is first to suggest that this circuit or some variant of it might be used in a PACSAT-like system to efficiently detect and locate the carrier frequency of a potential sender in order to establish a communication link. The bandwidth in which such a carrier can be is quite wide. Also the input signal-to-noise ratio of the carrier is only moderate. Hence a second purpose is to compute an estimate of the expected output signal-to-noise ratio for this detection criterion.

### SEMICOHERENT DETECTION AND LOCATION OF A CARRIER

To minimize the mathematical description of the semicoherent detection criterion, assume the unknown carrier signal is complex of form

$$s(t) = Ae^{i2\pi ft} = Ae^{i\omega t} \tag{A.1}$$

where $\omega = 2\pi f$ and f, the unknown carrier frequency, lies in the bandwidth interval,

$$\frac{-B}{2} < f < \frac{B}{2} \tag{A.2}$$

Physically, signal s(t) is obtained first by heterodyning a real sine wave $A\sin(2\pi ft)$ down in frequency so that the band of interest of bandwidth B is centered about zero frequency, as given by Eq. (A.2). The

*The symbols used in this appendix do not necessarily conform with those used in the text.

imaginary part of Eq. (A.1) is obtained as the quadrature component in the heterodyning process.

Accompanying any signal process must be a noise process. Originally this noise process is real but if the above heterodyning process is applied to the sum of the signal and the noise processes, one obtains the complex signal plus noise process,

$$w(t) = s(t) + z(t) = Ae^{i\omega t} + z(t), \tag{A.3}$$

where now both the signal $Ae^{i\omega t}$ and the noise process $z(t)$ lie in the bandwidth interval (Eq. (A.2)).

Assume the complex noise process

$$z(t) = x(t) + iy(t)$$

is the classical zero-mean Gaussian complex process where $y(t)$ is the Hilbert transform of $x(t)$. This is the usual process selected for an analysis of a communication channel. Also let

$$R(\tau) = E\left[z(t)\ \overline{z(t - \tau)}\right],$$

(where E denotes expected value operator and the bar denotes complex conjugate) be the covariance of the process $z(t)$ with itself, sometimes called the autocovariance of $z(t)$. It is well known that $R(\tau)$ is the inverse Fourier transform of the spectral density $G(f)$ of the process $z(t)$, i.e.,

$$R(\tau) = \int_{-\infty}^{\infty} e^{2\pi i f \tau}\ G(f)\ df$$

With these preliminaries, the semicoherent detection criterion for detecting the signal $Ae^{i\omega t}$ in noise $z(t)$ is

$$\left| \int_0^T w(t)\ \overline{w(t - \tau_o)}\ dt \right| \geq \text{const} \tag{A.4}$$

where w(t) is given by Eq. (A.3), T is called the integration time, and $\tau_o$ is a constant delay time to be chosen. If $t_o = 0$, then Eq. (A.4) becomes the classical energy detection criterion,

$$\int_0^T r^2(t)\, dt \geq \text{const} \tag{A.5}$$

where r(t) is the envelope process of w(t). The disadvantage of Eq. (A.5) over Eq. (A.4) is that all knowledge of the phase of the signal has been lost in the statistic

$$y = \int_0^T w(t)\, \overline{w(t - \tau_o)}\, dt \tag{A.6}$$

A better choice for $\tau_o$ is to choose $\tau_o$ so that the autocovariance of z(t) is zero, i.e.,

$$R(\tau_o) = 0, \tag{A.7}$$

or very nearly so. Taking the expected value of complex statistic y in Eq. (A.6) yields

$$E(y) = \int_0^T E\left[w(t)\, \overline{w(t - \tau_o)}\right] dt$$

$$= \int_0^T E\left[Ae^{i\omega t} + z(t)\right]\left[Ae^{-i\omega(t-\tau_o)} + \overline{z(t - \tau_o)}\right] dt$$

$$= \int_0^T E\left[A^2 e^{i\omega\tau_o} + Az(t)e^{-i\omega(t-\tau_o)} + A\overline{z(t - \tau_o)}e^{i\omega t} + z(t)\overline{z(t - \tau_o)}\right] dt$$

Using Eq. (A.7) and the fact that z(t) is zero mean, i.e.,

$$E\left[z(t)\right] = E\left[z(t - \tau_o)\right] = 0,$$

one obtains

$$E(y) = A^2 T e^{i\omega\tau_o} = A^2 T e^{2\pi i f \tau_o} \tag{A.8}$$

as the mean or expected value of statistic y. Observe in Eq. (A.8) that the frequency of the carrier can be obtained from the complex number E(y) by measuring the angle $2\pi f\tau_o$. Similarly, statistic y can be used to find an estimate of f. One such estimator for f is

$$\hat{f} = \frac{1}{2\pi\tau_o} \tan^{-1}\left(\frac{\text{Im } y}{\text{Re } y}\right) \tag{A.9}$$

where Re(y) and Im(y) are the real and imaginary parts of y.

The two hypotheses of the detection criterion in Eq. (A.4) are

$H_0$: $w(t) = z(t)$, the noise-only hypothesis

$H_1$: $w(t) = Ae^{i\omega t} + z(t)$, the signal-plus-noise hypothesis.

The semicoherent detection process in Eq. (A.4) uses a nonlinear statistic. Thus for the figure of merit of such a nonlinear statistic one can use an output signal-to-noise ratio of the form

$$(S/N)_o = \frac{|E_1(y) - E_0(y)|^2}{E_0|y - E_0(y)|^2} = \frac{|E_1(y) - E_0(y)|^2}{E_0|y|^2 - |E_0(y)|^2} \tag{A.10}$$

where $E_0(y)$ and $E_1(y)$ denote the conditional expectations

$$E_0(y) = E[y|H_0] \text{ and}$$

$$E_1(y) = E[y|H_1],$$

with respect to hypotheses $H_0$ and $H_1$, respectively.

To compute Eq. (A.10) for statistic y note first that

$$E_0(y) = 0 \tag{A.11}$$

and by Eq. (A.6) that

$$E_1(y) = A^2 T e^{i\omega\tau_o} \tag{A.12}$$

Hence

$$E_0|y - E_0(y)|^2 = E_0|y|^2 \tag{A.13}$$

To find $E_0|y|^2$ in Eq. (A.13) in a simple manner it is desirable to use some approximations. Let the integral for y in Eq. (A.6) be approximated by a Riemann sum as follows

$$\begin{aligned} y &= \int_0^T z(t)\ \overline{z(t - \tau_o)}\ d\tau \\ &\approx \sum_{k=1}^{n} z(k\Delta)\ \overline{z(k - p)\Delta} \end{aligned} \tag{A.14}$$

where $\Delta$ is the reciprocal of the bandwidth B, i.e.,

$$\Delta = \frac{1}{B} \tag{A.15}$$

$$T = n\Delta$$

and p is the least integer greater than

$$\frac{\tau_o}{\Delta} = \tau_o B$$

or (A.16)

$$p = [\tau_o B]$$

the so-called principal part of number $\tau_o B$. Let the spectrum of $z(t)$ be zero outside the interval $-B \leq f \leq B$. That is, assume the spectrum is band-limited. Then

$$R(\Delta) = R(1/B) = 0 \tag{A.17}$$

Letting $z(k\Delta) = z_k$, then Eq. (A.17) yields

$$E\left[z_k \overline{z}_j\right] = 2\sigma^2 \delta_{ij} \tag{A.18}$$

where

$$\sigma^2 = E(\text{Re } z_k^2) = E(\text{Im } z_k^2)$$

and $\delta_{ij}$ is the Kroneker delta function with

$$\delta_{ij} = \begin{cases} 1 & i = j \\ 0 & i \neq j \end{cases}$$

Putting the sum approximation (Eq. (A.14)) in Eq. (A.13) produces

$$E_0|y|^2 = \Delta^2 \sum_{k=1}^{n}\sum_{j=1}^{n} E\left(z_k \bar{z}_{k-p}\ \bar{z}_j z_{j-p}\right) \tag{A.19}$$

Since the $z_k$'s are jointly Gaussian, one may use the identity [A.4],

$$E(z_1\bar{z}_2 z_3\bar{z}_4) = E(z_1\bar{z}_2)\ E(z_3\bar{z}_4) + E(z_1\bar{z}_4)\ E(z_3\bar{z}_2),$$

on Eq. (A.19), thereby obtaining

$$E_0|y|^2 = \Delta^2 \sum_{j=1}^{n}\sum_{k=1}^{n} \left\{ E\left(z_k z_{k-p}\right)\ E\left(\bar{z}_j z_{j-p}\right) + E\left(z_k \bar{z}_j\right) E\left(\bar{z}_{k-p}\ z_{j-p}\right)\right\} \tag{A.20}$$

This latter expression is readily evaluated with Eq. (A.18) to yield finally

$$E_0|y|^2 = \Delta^2 \sum_{k=1}^{n} \left(2\sigma^2\right)^2 = \Delta T \left(2\sigma^2\right)^2 \tag{A.21}$$

If one substitutes Eqs. (A.11, A.12, and A.21),

$$(S/N)_o = \frac{\left|A^2 e^{i\omega\tau_o}\right|^2}{\Delta T (2\sigma^2)^2} = \left(\frac{A^2}{2\sigma^2}\right)^2 \frac{T}{\Delta} = (S/N)_i^2\ BT \tag{A.22}$$

as the output signal-to-noise ratio in terms of the usual input signal-to-noise

$$(S/N)_i = \frac{A^2}{2\sigma^2}$$

This result is the same figure of merit measure that is usually obtained for the classical square law or power detector criteria [5].

SOME ADDITIONAL REMARKS

At the suggestion of the author of this appendix, the semicoherent criterion or autocovariance was tested and applied to long pulse detection by John L. Allen [5] at the MIT Lincoln Laboratory in 1959. John Allen's circuit was attached to the receiver of the 400 megahertz experimental satellite detection radar at Millstone Hill, Massachusetts.

The Millstone radar had a long cw pulse about one millisecond in duration. The doppler filter bank to cover the doppler band of interest required about 512 analog filters, overlapping at the three decibel level, with each filter matched to a one millisecond pulse. The semicoherent detection circuit was put in parallel with this filter bank for comparative evaluation.

For the same measured false-alarm rate, the autocovariance detection and doppler estimation circuit appeared to perform almost as well as the doppler filter bank system in terms of probability of satellite detection. Every time the filter bank detected a satellite, John Allen's circuit also made a detection.

Other more pressing matters and the vicissitudes of the time made it difficult to accomplish carefully controlled experiments with semicoherent detection on the Millstone Hill radar. For one thing, the increased number of satellites made this radar an operational radar, rather than an experimental tool of the laboratory. Finally, because of the analog nature and complexity of the filter bank, its performance would vary almost on a daily basis, making any comparison with another detection criterion uncertain at best. In spite of these deficiencies in the experiment, the informal results seem to indicate that semicoherent detection is qualitatively comparable in terms of probability of detection with a fixed false-alarm rate to square law detection.

The semicoherent detector can be implemented at the complex video level, or at the output of the I.F. section of the radar receiver. John Allen's original circuit was realized by the latter approach using mixers and analog delay lines and integrators. A simplified block diagram of this circuit is shown in Fig. A.1.

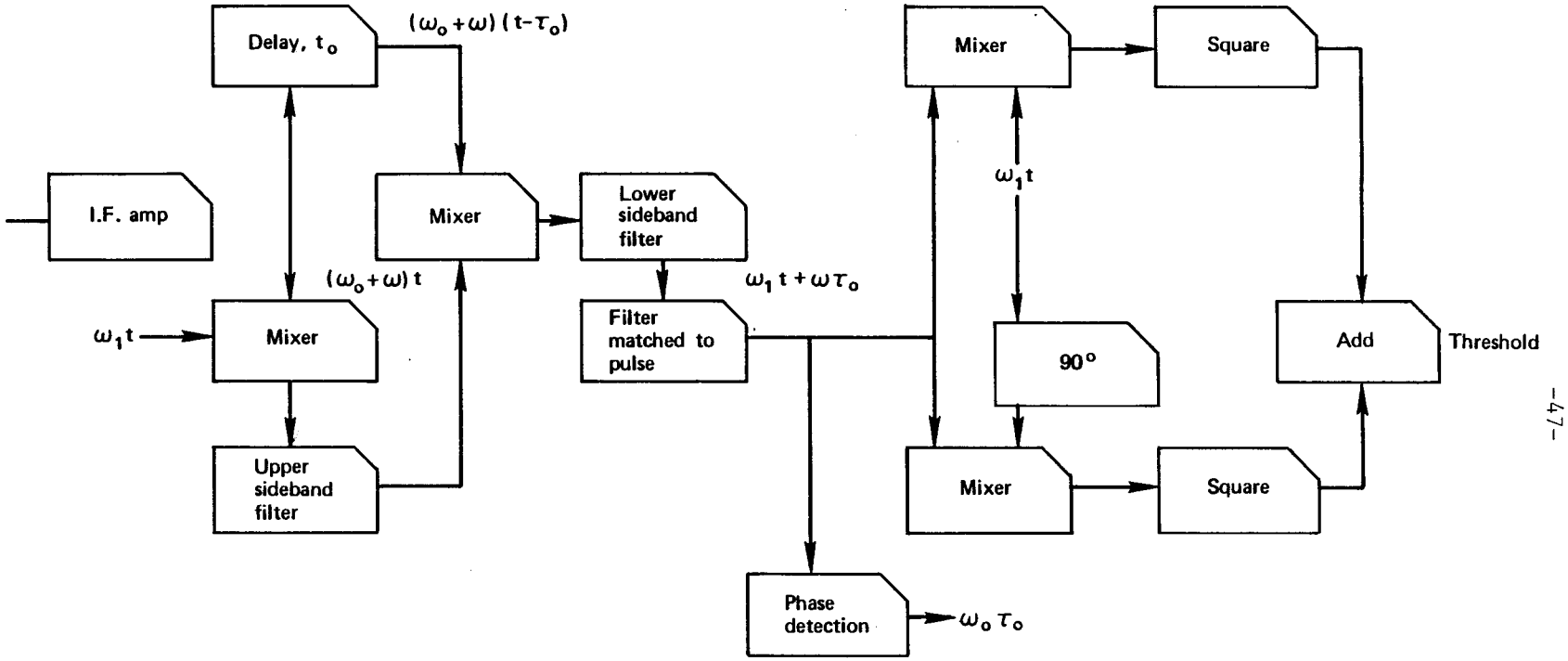


Fig. A-1 — Simplified block diagram of a semicoherent detector operating on an I.F. waveform (the phases of noise-free signals are indicated at different points in the diagram)

## REFERENCES TO THE APPENDIX

1. Reed, I. S., *The Autocovariance Filter*, MIT Lincoln Laboratory Group Report, GR-47.14, 23 January 1958.

2. Reed, I. S., *Semi-Coherent Detection*, The Rand Corporation, P-2106, 19 September 1960.

3. Lank, G. W., I. S. Reed, and G. E. Pollon, "A Semicoherent Detection and Doppler Estimation Statistic," *IEEE Trans. on Aerospace and Electronic Systems*, Vol. AES-9, No. 2, March 1973.

4. Reed, I. S., "On a Moment Theorem for Complex Gaussian Processes," *IEEE Trans. on Information Theory*, Vol. IT-8, No. 3, April 1962.

5. Allen, J. L., *The Autocovariance Filter*, MIT Lincoln Laboratory Group Report, GR-31-150, 10 August 1959.